

# Complex ordering in spin networks: Critical role of adaptation rate for dynamically evolving interactions

Anand Pathak\* and Sitabhra Sinha†

*The Institute of Mathematical Sciences, CIT Campus, Taramani, Chennai 600113, India.*

(Dated: April 30, 2019)

Many complex systems can be represented as networks of dynamical elements whose states evolve in response to interactions with neighboring elements, noise and external stimuli. The collective behavior of such systems can exhibit remarkable ordering phenomena such as *chimera order* corresponding to coexistence of ordered and disordered regions. Often, the interactions in such systems can also evolve over time responding to changes in the dynamical states of the elements. Link adaptation inspired by Hebbian learning, the dominant paradigm for neuronal plasticity, has been earlier shown to result in structural balance by removing any initial frustration in a system that arises through conflicting interactions. Here we show that the rate of the adaptive dynamics for the interactions is crucial in deciding the emergence of different ordering behavior (including chimera) and frustration in networks of Ising spins. In particular, we observe that small changes in the link adaptation rate about a critical value result in the system exhibiting radically different energy landscapes, viz., smooth landscape corresponding to balanced systems seen for fast learning, and rugged landscapes corresponding to frustrated systems seen for slow learning.

## I. INTRODUCTION

Many natural and technological complex systems can be described as networks connecting a large number of elements whose states evolve in time [1, 2]. The collective behavior of a system resulting from interactions between its components can exhibit non-trivial features, including critical phenomena [3]. For instance, a system of binary-state elements (e.g., representing individuals having opposing opinions on an issue) connected through a network having modular organization can exhibit ordering dynamics at very distinct time-scales [4] and under certain circumstances, self-organize into locally aligned clusters that correspond to the communities of the network (i.e., subnetworks characterized by a significantly higher connection density compared to the overall density of the network) [5]. In many situations, the links of the network (representing the interactions) can also evolve over time as a result of the changes in the states of the components that they connect. Such connections may not only be characterized by weights (indicating the strength of interaction) but also sign (representing the nature of the interaction). For instance, in the context of a network of synaptically-connected model neurons, positive links may correspond to excitatory interactions (whereby activation of one element can result in activation of other connected elements) while negative links can give rise to inhibition (i.e., activation of an element tends to suppress subsequent activation of neighboring elements) [6].

The occurrence of negative links can lead to the emergence of *frustration* because of the existence of inconsistent relations within cycles in the network [7, 8]. A network is said to be structurally balanced if its positive and

negative links are arranged such that frustration is absent. Such a network can always be represented as two communities, with interactions within each community being exclusively positive while those between communities can only be negative [9]. This is of interest not only for social systems in the context of which the concept of balance was first introduced [10], but also for biological systems. For instance, it has been recently observed that the resting human brain is organized into a pair of dynamically anti-correlated subnetworks [11]. This suggests that the network responsible for this behavior may be structurally balanced. This possibility is intriguing in view of the observation of non-trivial collective behavior in balanced networks of binary-state dynamical elements, such as, the coexistence of ordered and disordered regions referred to as “chimera” order, in the presence of an external field [12]. The process by which networks can evolve to a balanced configuration has been explored by considering a link adaptation process inspired by Hebb’s principle, the basis behind neural plasticity [13]. According to this mechanism, weights associated with each link change in proportion to the correlation in the activity of the connected elements. Therefore, any initial frustration in the network can be removed by modifying the connection weights in accordance with the dynamical states of the elements. Systems undergoing such link adaptation in the presence of environmental noise show high variability in the convergence time required to reach the balanced state [14].

In this paper we consider how the rate of dynamical evolution of interactions in accordance with the Hebbian adaptation principle affects the collective behavior of the network. Starting from a fully connected network that is structurally balanced and introducing noise and external field so that the system exhibits chimera order, we show that different rates of adaptation can result in distinct outcomes. Fast learning rates result in persistence of the chimera regime, although the balanced network now

\* anandp@imsc.res.in

† sitabhra@imsc.res.in

comprises communities with asymmetric sizes, viz., the ordered sub-network containing a much larger fraction of elements of the network. Slow learning, on the other hand, results in a completely ordered state with the interactions becoming only of positive nature. On removing the external field, fast learning results in retrieving a network that is similar to the original one, i.e., structurally balanced with communities of almost equal size. However, slow learning gives rise to a fully frustrated network exhibiting disorder. We observe that there exists a critical interval for values of the learning rate, around which small changes result in the system converging to distinct final states. In the following sections we first discuss the model and adaptation dynamics, followed by description of the results of numerical simulations. We conclude with a brief summary of our results and a discussion of their implications.

## II. THE MODEL

For the purpose of investigating how collective behavior of a complex system is affected by adaptive dynamics of interactions, we use one of the well-known spin models of statistical physics which are generic systems for analyzing cooperative phenomena. In particular, we use the binary-state Ising spin, the spin orientations (“up” or “down”) representing a pair of mutually exclusive choices. The simplicity of the model makes it applicable to not just magnetic materials (in the context of which it was originally proposed) but any system where the elements choose between the two competing states based on interactions with neighboring elements, noise (represented by thermal fluctuations characterized by a temperature  $T$ ) and external stimulus (often represented by a magnetic field  $H$ ). The interactions  $J_{ij}$  between any pair of spins ( $i, j$ ) can be either positive (promoting connected spins to have the same state) or negative (promoting connected spins to have opposite states) in nature. For instance, in neuronal networks, one can view the neurons as binary-state devices that are either firing (active) or quiescent (inactive). Correspondingly, as pointed out earlier, the excitatory and inhibitory connections between neurons can be represented by positive and negative interactions, respectively. At a different scale, one can view genetic regulatory networks in a similar vein, with genes being in either of two states, viz., getting expressed (active) or not (inactive). In this setting, genes promoting the expression of other genes correspond to positive interaction, while inhibiting the expression of other genes correspond to negative interactions. In a different context, the interactions between Ising spins can also be used to represent social intercourse [15]. Here, the spin states are considered to be analogous to two competing opinions, while the interactions may represent the nature of the relation between a pair of individuals - positive corresponding to affiliative and negative corresponding to antagonistic relations.

We consider a system of  $2N$  globally coupled Ising spins arranged into two sub-populations (called modules or communities) each having  $N$  spins, at a constant temperature  $T$ . For the simulations reported below we have chosen  $N = 100$ . The interaction between a pair of spins belonging to the same module is positive having strength  $J (> 0)$ , while that between spins belonging to different modules is negative with strength  $-J'$  (where  $J' > 0$ ). In the absence of an external field and thermal fluctuations (i.e.,  $H = 0, T = 0$ ), the two modules will be completely ordered in opposite orientations. When subjected to an external field of strength  $H$ , the energy of the system is described by

$$E = -J \sum_{i,j,\alpha} \sigma_{i\alpha} \sigma_{j\alpha} - J' \sum_{i,j,\alpha,\beta} \sigma_{i\alpha} \sigma_{j\beta} - H \sum_{i,\alpha} \sigma_{i\alpha}, \quad (1)$$

where  $\sigma_{i\alpha} = \pm 1$  is the Ising spin on the  $i$ -th node ( $i, j = 1, 2, \dots, N$ ) in the  $\alpha$ -th module ( $\alpha, \beta = 1, 2$ ). As every spin interacts with every other spin, a mean-field treatment should describe the system accurately. For convenience we define  $a = J(N - 1)/2$  and  $b = J'N$  as system parameters. The state of all spins in the system are updated stochastically at discrete time-steps using the Metropolis Monte Carlo (MC) algorithm with temperature  $T$  expressed in units of  $k_B T/J$  where  $k_B$  is the Boltzmann constant. The initial state of the system we have chosen is one exhibiting chimera order [12], to obtain which we use  $a = 1, b = H = 10$  and  $k_B T/J = 5$ .

We also allow the possibility that the interaction strengths can change over time through an adaptation process inspired by the principle of Hebbian learning, a classical concept in the area of neural networks [13]. Colloquially often described as “neurons that fire together, wire together”, in this mechanism the strength of synaptic connection between a pair of neurons is incremented when the two exhibit correlated activation. In Ref. [14], this idea was used to propose a link adaptation rule that applies to a system of spins coupled via positive, as well as, negative interactions as:

$$J_{ij}(t+1) = (1 - \epsilon)J_{ij}(t) + \epsilon \sigma_i(t)\sigma_j(t), \quad (2)$$

which is applied after every MC step. The adaptation rate,  $\epsilon$ , decides the time-scale over which the interaction strength changes relative to the spin dynamics. Starting with an initially frustrated spin system, implementing the above  $J_{ij}$  dynamics in absence of thermal fluctuations (i.e.,  $T = 0$ ) results in the system converging to a structurally balanced state [14]. This can be intuitively understood in terms of changes in the energy landscape over which the state of the spin system evolves. Frustrated systems have rugged energy landscapes comprising a large number of local minima (a fact which is exploited in neural network models of associative memory where these minima are used to embed desired patterns one wishes the network to “memorize” [16, 17]). Thus, beginning at any randomly chosen initial state of spin configurations, the spin dynamics drives the system into

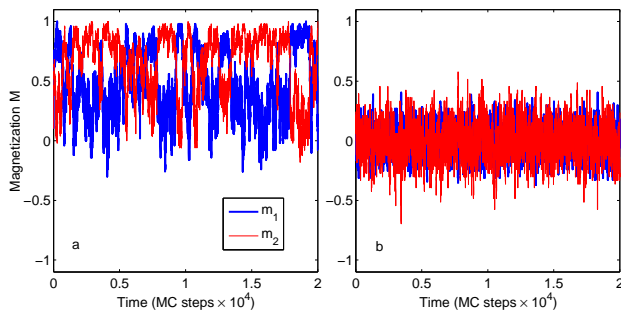


FIG. 1. Typical time-evolution of the magnetizations per spin of the two modules,  $m_1$  and  $m_2$ , in (a) chimera ordered state and (b) disordered state, shown for MC simulations with  $N = 100$  at (a)  $k_B T/J = 5$  and (b)  $k_B T/J = 8$ , respectively.

the nearest local energy minimum. The subsequent evolution of the  $J_{ij}$ s converts this into the global minimum of the system. However, in the presence of noise ( $T > 0$ ), fluctuations in the spin dynamics can prevent the system from being trapped in any state for sufficiently long duration. Thus, the adaptation dynamics fails to alter the energy landscape sufficiently so as to turn the configuration into the global minimum. Therefore, with increasing temperature, an extremely long time may be required to reach structural balance.

In this paper we use a modified form of the Hebb-inspired adaptation rule for interaction strengths that was introduced in Ref. [14]. This is to take into account the asymmetry in the strengths of positive and negative interactions necessary for observing chimera order (typically  $J' \simeq 10J$ ) [12]. We change the adaptation rule such that the upper and lower bounds for the evolving interactions have the same values as that of the positive and negative interactions (respectively) which give rise to the chimera ordered state. Thus after each MC step, interaction strengths are changed according to:

$$J_{ij}(t+1) = J_{ij}(1 - \epsilon) + \epsilon[(J + J')\frac{\sigma_i \sigma_j}{2} + \frac{1}{2}(J - J')]. \quad (3)$$

The state of the system at any time is characterized by two quantities. One of these is the frustration associated with the interactions, measured by calculating the fraction of frustrated triads (i.e., connected sets of 3 spins with an odd number of negative interactions) in the system:

$$F = \sum_{i \neq j \neq k} \frac{J_{ij} J_{jk} J_{ki}}{N C_3}, \quad \forall J_{ij} J_{jk} J_{ki} < 0, \quad (4)$$

which varies between 0 (no frustration) and 1 (completely frustrated).

The other quantity is an order parameter  $p = |m_1 - m_2|$  that is used to identify a chimera state in a spin system with two modules that have magnetizations  $m_1$  and  $m_2$ , respectively. To numerically estimate the order parameter  $p$ , we are confronted with a few potential complications. First, as the magnetizations of the two modules

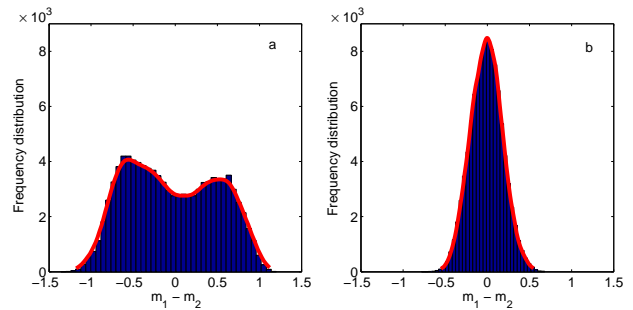


FIG. 2. Frequency distribution of the quantity  $m_1 - m_2$  shown when the spin system exhibits (a) chimera order and (b) disorder. The kernel smoothed distribution function is represented by a thick curve. Results shown for MC simulations with  $N = 100$  at (a)  $k_B T/J = 5$  and (b)  $k_B T/J = 8$ , respectively.

are stochastically fluctuating (especially the one which is disordered, i.e., having lower magnetization), we can use their average values. However, this gives rise to an additional problem as the modules can frequently exchange their order/disorder status, especially when the modules are of the same size [Fig. 1 (a)]. Thus, a method is required to measure  $p$  that is unaffected by the modules switching their magnetizations, while being able to determine if the time-averaged magnetizations of the two modules are different (the signature of chimera order). For instance, a simple time average of the absolute value of differences between  $m_1$  and  $m_2$  will not give correct results as one obtains a finite value (because of stochastic fluctuations) even when the time averaged magnetizations are same for both modules [Fig. 1 (b)]. Therefore, to estimate  $p$  we have used the following algorithm. First, the frequency distribution of  $m_1 - m_2$  is computed. In the absence of chimera, the distribution is unimodal [Fig. 2(a)] which is approximated as a Gaussian function, while for chimera ordering the distribution is bimodal [Fig. 2(b)] which is approximated as a superposition of two Gaussian functions. For a unimodal distribution, the value of  $m_1 - m_2$  corresponding to the peak is used to calculate the order parameter  $p$ . For bimodal distributions, a weighted average of the values corresponding to the peaks is used. For example, if one of the peaks occurs at  $p_1$  with value  $h_1$  while the other is at  $p_2$  with value  $h_2$ , the order parameter is calculated as  $p = (h_1|p_1| + h_2|p_2|)/(h_1 + h_2)$ . In order to make the automated detection of the peak locations accurate, the frequency distributions need to be smoothed of all fluctuations in the frequencies so that the local maxima at the peaks can be uniquely determined. For this purpose we have used a kernel smoothing technique [18] that gives a single peak location for unimodal distributions and locations for two peaks in the case of bimodal distributions.

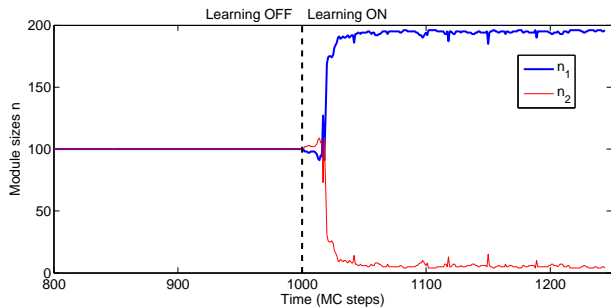


FIG. 3. Time-evolution of sizes of the modules resulting from link adaptation dynamics that is introduced at time  $t = 1000$  MC steps (indicated by broken line). The ordered module expands in size ( $n_1$ ) while the disordered one shrinks. Learning rate  $\epsilon = 0.1$

### III. RESULTS

Starting from a structurally balanced network comprising two modules, we first introduce field and thermal fluctuations so as to drive the system into chimera order - i.e., one of the modules becomes ordered while the other is disordered. Once this is achieved we allow adaptation dynamics of the interactions to take place. As the evolution of the interactions are related to the degree of fluctuations in the spin states, these would occur mostly in the disordered module where the spins are subject to the competing forces of negative interactions with the spins belonging to the ordered module and the influence exerted by the uniform external magnetic field which tries to align the spins in parallel with those of the ordered module. Thus, at any instant, a few spins in the disordered module will get aligned with the spins in the other module and consequently may develop positive interactions with the latter as a result of link adaptation. This means that they will now no longer be part of the disordered module but become part of the ordered module. As a result, the size of the modules would change over time - the ordered module increasing at the expense of the disordered one. This has to be taken into account when measuring system properties, such as, magnetization per spin of the two modules. In order to have a consistent definition of module size that would be valid even when the system is no longer in structural balance, we heuristically measure it as follows. At each update of the  $J_{ij}$ s, we randomly choose a spin from the ordered module and consider all spins that have positive interactions with it to belong to the ordered module, with the remaining spins comprising the disordered module. Following this process, we can follow the time-evolution of modular membership of individual spins, as well as, that of the module sizes. However, this measure becomes less useful as the system becomes increasingly frustrated.

Fig. 3 illustrates the evolution of module sizes with time following the introduction of link adaptation dynamics in the system. We can now measure the magnetizations per spin,  $m_1$  and  $m_2$ , of the two modules

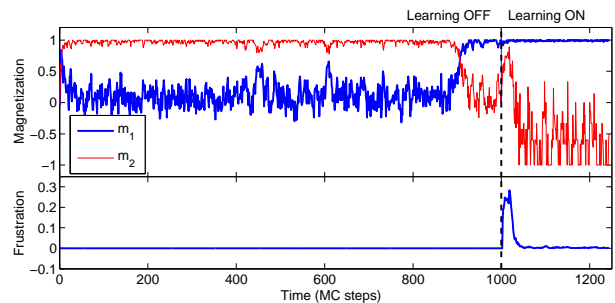


FIG. 4. (top) Time-evolution of magnetizations  $m_1$  and  $m_2$  of the two modules in the network (having sizes  $n_1$  and  $n_2$ , respectively) before and after link adaptation dynamics is introduced at time  $t = 1000$  MC steps (indicated by broken line). In absence of adaptation, magnetizations show the characteristic signature for chimera order. Once adaptation dynamics is operational, the ordered module with magnetization  $m_1$  is seen to increase in size. (bottom) In absence of learning, the network exhibits no frustration as it is structurally balanced. Following the introduction of adaptation dynamics, there is a transient increase in frustration, before the system once again achieves balance, but with modules of asymmetric sizes.

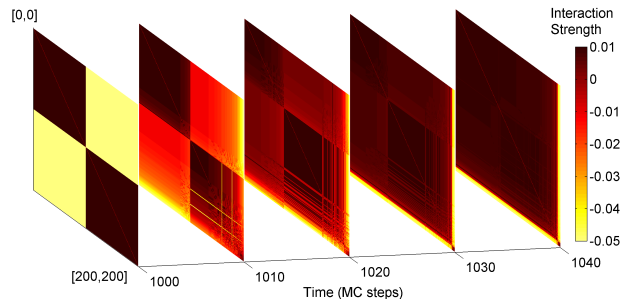


FIG. 5. Snapshots of the time-evolution of the interaction matrix  $\mathbf{J}$  after adaptation dynamics is initiated at  $t = 1000$  MC steps. Note that the time interval shown here corresponds to the same period over which the frustration in the system initially rises and then decreases again as the system once more reaches a balanced state, as indicated in Fig. 4.

by taking into account the modular membership of each spin and the module sizes. Fig. 4 shows these order parameters, as well as, the frustration in the network, as a function of time before and after the link adaptation dynamics is introduced. As expected, we observe that following the start of link adaptation dynamics, the ordered module begins to grow in size, which is also observed in the time-evolution of the interaction matrix (shown as snapshots at regular intervals in Fig. 5).

The time-evolution of the initial chimera-ordered network subjected to link adaptation dynamics with various learning rates ranging from  $\epsilon = 0.1$  to  $10^{-4}$  are indicated in Figs. 6-9. For fast learning rates (e.g.,  $\epsilon = 0.1$ ), the system immediately converges to a balanced state characterized by a large ordered module (comprising about 95% of all the elements) and a small disordered one. By observing the magnetization time-series of the two modules in Fig. 6 it is easy to infer that the system still exhibits chimera order. We note that a rise in frustration

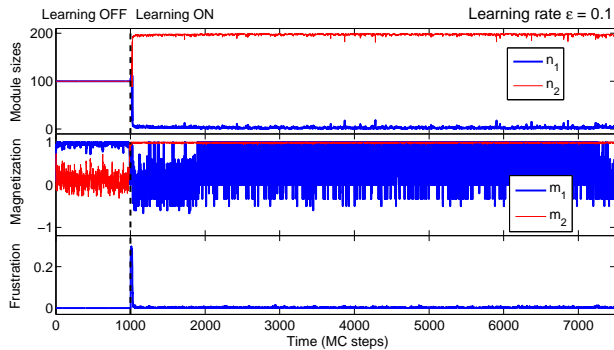


FIG. 6. Time-evolution of module sizes (top panel), magnetization (middle panel) and frustration (bottom panel) for an initially chimera ordered system in the presence of an external field before and after link adaptation dynamics with rate  $\epsilon = 0.1$  is introduced (the time at which the link adaptation is initiated is indicated by the broken line). Following a brief transient rise in the frustration, the system again attains a balanced state although with asymmetric module sizes.

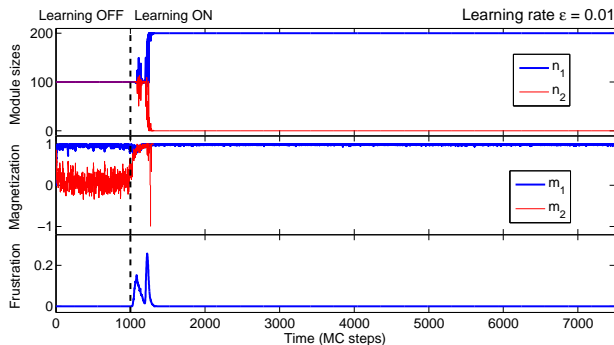


FIG. 7. Time-evolution of module sizes (top panel), magnetization (middle panel) and frustration (bottom panel) for an initially chimera ordered system in the presence of an external field before and after link adaptation dynamics with rate  $\epsilon = 0.01$  is introduced (the time at which the link adaptation is initiated is indicated by the broken line). The system eventually becomes completely ordered with all interactions becoming positive (resulting in merging of the two modules into a single one).

is seen for a very brief duration during the initial period immediately following initiation of the link adaptation dynamics. For a slower learning rate, viz.  $\epsilon = 0.01$ , the process of expansion in size of the ordered module is different (Fig. 7). We notice that soon after the beginning of link adaptation, the chimera ordering is lost as the disordered module becomes ordered. However, the modules still retain their different identities as they are defined based on the sign of interactions of the spins within them (which should be positive) and that with spins in the other module (which should be negative). For even slower learning rates such as  $\epsilon = 10^{-3}$  or  $10^{-4}$  (Figs. 8-9) the duration over which the two modules exist while both being ordered is seen to increase. During this period the modular membership of the spins do not change significantly (apart from small fluctuations). Chimera ordering is lost as the interaction strengths for spins in the

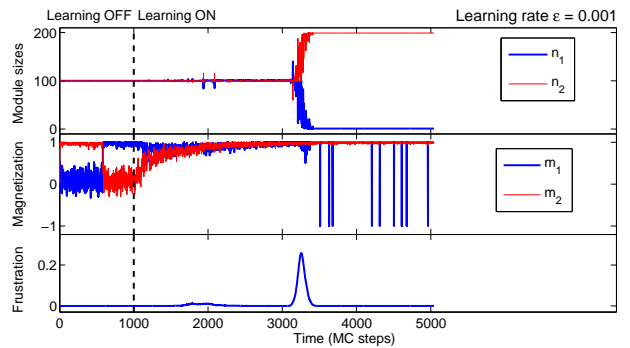


FIG. 8. Time-evolution of module sizes (top panel), magnetization (middle panel) and frustration (bottom panel) for an initially chimera ordered system in the presence of an external field before and after link adaptation dynamics with rate  $\epsilon = 10^{-3}$  is introduced (the time at which the link adaptation is initiated is indicated by the broken line). Initially, the two modules both become ordered. However, eventually the two modules merge into a single one as all interactions become positive. The time of merging coincides with the transient rise in frustration.

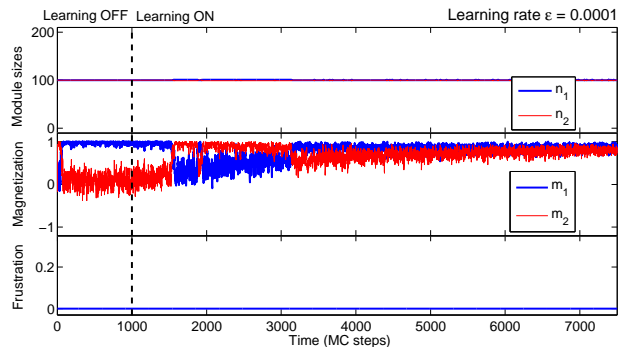


FIG. 9. Time-evolution of module sizes (top panel), magnetization (middle panel) and frustration (bottom panel) for an initially chimera ordered system in the presence of an external field before and after link adaptation dynamics with rate  $\epsilon = 10^{-4}$  is introduced (the time at which the link adaptation is initiated is indicated by the broken line). We observe that while one of the modules remains ordered, the initially disordered module is gradually also tending towards complete order. Eventually one expects the two modules to merge into a single one.

disordered module becomes weaker as a result of frequent switchings of their orientations. As a result the effect of the external field becomes dominant, which causes the spins in the disordered module to align with it. As spins in both modules are now aligned parallel to each other, adaptation of their interactions with time would eventually make all interactions positive, thereby merging the two modules into one. The time at which this happens is indicated by a transient rise in the frustration (Figs. 7 and 8), occurring much later for slower rates of adaptation.

The different scenarios we observe at fast and slow learning rates suggest that there is a competition between two processes: if the modular membership of the spins can change rapidly following initiation of link adaptation

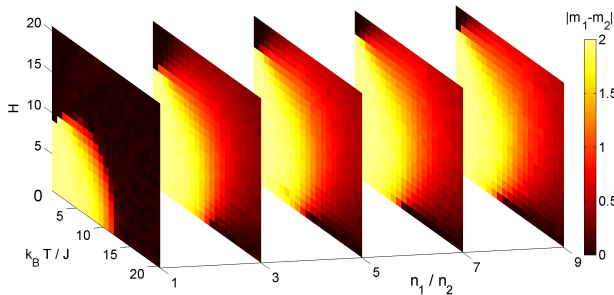


FIG. 10. The region of chimera order in the  $(H, T)$  parameter space shown for different ratios of the sizes of the two modules. Chimera is indicated in terms of high values of the order parameter  $|m_1 - m_2|$  (represented by different colors).

so that the system adopts a new structurally balanced configuration, the interaction strengths of the spins in the disordered module do not decrease significantly - thereby allowing the two modules to coexist with the chimera ordering intact (although the modules now have very different sizes). Note that the modular membership of the spins will change rapidly as they continually change their interaction strengths because of the fast adaptation rate. However, the average number of spins in each module will remain fairly steady. If the learning rate is slow, the interaction strengths will not have time to change sufficiently rapidly to allow the system to reach a new structurally balanced state following the initiation of link adaptation dynamics. As a result the field dominates over the weakened interactions of the spins in the disordered module, thereby eliminating chimera order and eventually causing the two modules to merge.

The existence of chimera order even in situations where the two modules have very different sizes is a novel observation as earlier it had only been observed in a system with symmetric module sizes [12]. In order to see how the region in the field-temperature parameter space where we observe chimera ordering varies with asymmetry in the module sizes, we show in Fig. 10 the dependence of the order parameter  $|m_1 - m_2|$  on the strength of the external field  $(H)$ , the scaled temperature  $(k_B T / J)$  and the ratio of sizes of the two modules  $(n_1 / n_2)$  in the absence of link adaptation dynamics. We observe that the region in parameter space where we find chimera order (higher values of  $|m_1 - m_2|$ ) increases significantly as we go towards higher module size ratios (i.e.,  $n_1 / n_2$ ) especially for lower values of temperature.

We now consider the situation when the external field is withdrawn while allowing the link adaptation dynamics to continue. A difference is expected with the results shown in the earlier work [14] where the effect of link adaptation on the evolution of a system subject to thermal fluctuations was investigated, as the learning rule is different on account of the asymmetry in the strengths allowed for negative and positive interactions. As the adaptation dynamics used here allows for much stronger negative interactions (as compared to positive), we would

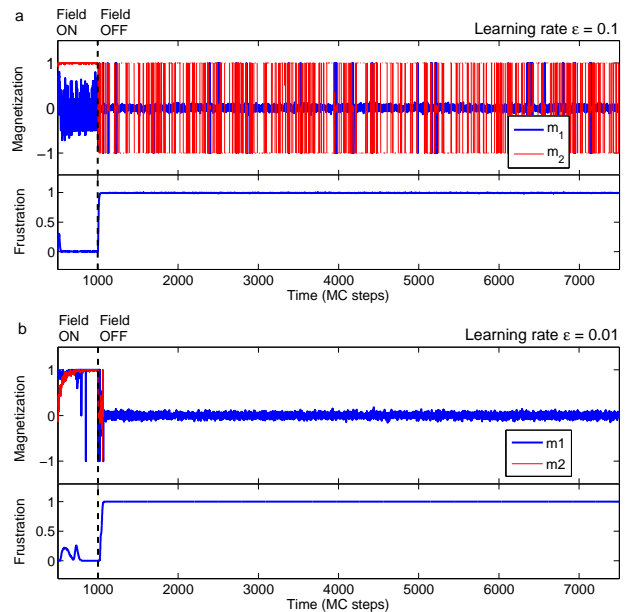


FIG. 11. (a) Time-evolution of magnetization (top panel) and frustration (bottom panel) for an initially chimera ordered system with link adaptation rate  $\epsilon = 0.1$ , before and after an external field is withdrawn (the time at which the field is switched off is indicated by the broken line). We observe that the system becomes completely frustrated on withdrawal of the field. (b) The corresponding time-evolution shown for link adaptation rate  $\epsilon = 0.01$ .

expect the system to become more frustrated as negative interactions are much more likely to contribute frustrated triads. This is indeed what is observed for slow learning rates, e.g.,  $\epsilon = 0.1$  and  $\epsilon = 0.01$  (Fig. 11). Note that in a frustrated system, one cannot define modules in a meaningful way, and thus the distinction between modules indicated in the time-series for magnetization is an artifact of the measurement method. For both of the slow learning rates we observe that the system converges to a fully frustrated state corresponding to the maximum value of the measure of frustration in the system ( $= 1$ ).

For faster link adaptation rates, however, we observe unexpected behavior in the system. For a learning rate  $\epsilon = 0.13$  [Fig. 12], which is only slightly higher than  $\epsilon = 0.1$  [shown in Fig. 11 (a)], the system initially becomes fully frustrated after the external field is withdrawn. Surprisingly, after a period of  $\sim 2000$  MC steps during which the system remains frustrated, it suddenly converges to a balanced state. This intervening period between the field being switched off and the system spontaneously splitting into two modules having positive interactions among all elements within them (and correspondingly, negative interactions between elements belonging to different modules) becomes even shorter with increasing learning rates (e.g., see Fig. 13 for  $\epsilon = 0.15$ ). Thus, we can identify a critical value of around 0.13 for the link adaptation rate  $\epsilon$ , below which the system remains frustrated and above which the system converges to a balanced state, on withdrawal of the external field.

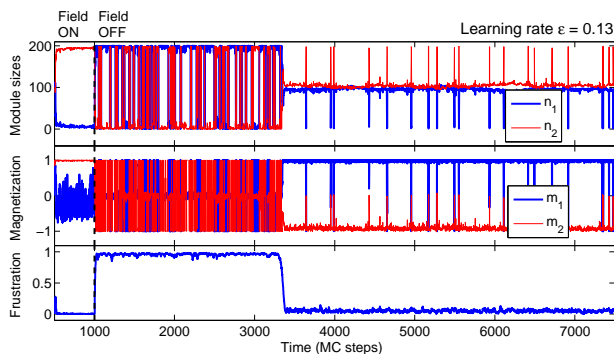


FIG. 12. Time-evolution of module sizes (top panel), magnetization (middle panel) and frustration (bottom panel) for an initially chimera ordered system with link adaptation rate  $\epsilon = 0.13$ , before and after an external field is withdrawn (the time at which the field is switched off is indicated by the broken line). We observe that the system initially becomes completely frustrated on withdrawal of the field. However after about 2000 MC steps the system suddenly becomes balanced.

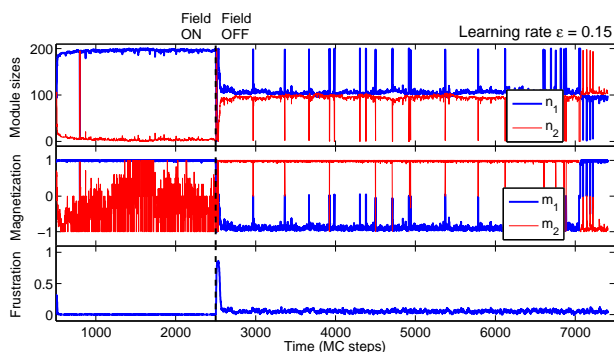


FIG. 13. Time-evolution of module sizes (top panel), magnetization (middle panel) and frustration (bottom panel) for an initially chimera ordered system with link adaptation rate  $\epsilon = 0.15$ , before and after an external field is withdrawn (the time at which the field is switched off is indicated by the broken line). We observe that the system quickly becomes balanced after a brief transient rise in frustration following the withdrawal of the field.

Indeed our simulations show that at  $\epsilon = 0.13$  there is a wide variation in the time required for the system to converge to balance after the field is switched off.

In the previous study of structural balance [14], it had been observed that the time required to converge to a structurally balanced state exhibits a bimodal distribution for a range of temperatures. We observe similar features in our model also - for instance, for a link adaptation rate of  $\epsilon = 0.13$ . For slightly slower learning rates (e.g.,  $\epsilon = 0.12$ ), the convergence time increases significantly. In our simulations, many realizations did not converge to the balanced state within the time of observation ( $10^4$  MC steps). For higher learning rates, the system rapidly converges to balance. However, unlike the convergence to balance seen in the previous study [14], the modules in the structurally balanced state that our model system reaches are of almost equal size (see Figs. 12 and 13) independent of the initial state of the network (in-

cluding the initial distribution of interactions which was seen to affect the nature of the balanced state that the system converges to in the earlier work). This may appear surprising as starting from a balanced state, one expects that the network will remain in that state as the interactions adapt so as to make the corresponding energy minimum even deeper. However, what we observe is that, on withdrawing the field the balanced state characterized by asymmetric module sizes is destabilized and the energy minimum moves in the configuration space eventually reaching the region corresponding to balanced state with modules having equal size. This difference between our results and that of the previous study suggests that the adaptation rule used here (which is biased in favor of negative interactions) is responsible for an intriguing meta-dynamics of the energy landscape itself.

We have also observed how the structure of the energy landscape underlying our system evolves as the interactions change through the adaptation rule. In the model studied earlier [14], the frustration of the initially disordered system is around 0.5. On initiating link adaptation, this value decreases as the system tends towards balance. When frustration reaches a value around 0.49, we observe that the energy landscape becomes such that starting from any spin configuration one can reach the same minimum energy spin arrangement. This suggests that a small decrease in the frustration can accompany a very large change in the basin of attraction of an energy minimum (which now encompasses a significant fraction of the configuration space). We observe similar behavior in our model system where the adaptation occurs in the presence and subsequent absence of an external field. For example, for an adaptation rate of  $\epsilon = 0.13$ , when the field is withdrawn the system initially becomes completely frustrated with the value of frustration measured as around 0.97. The corresponding energy landscape has a very large number of minima, each having very small basins of attraction. As the system evolves towards a balanced state, we note that even when the frustration decreases by a very small amount, e.g., to 0.93, the energy landscape transforms to one having an extremely deep energy minimum with a very large basin of attraction. We believe that this radical transformation of the energy landscape of the system at the initial stages of approach to balance points to features of landscape evolution that deserve further study.

#### IV. CONCLUSIONS

In this paper we have explored the behavior of a spin system that is subjected to an external field, while the interactions adapt in response to the system dynamics. The results obtained through our simulations that is described above is summarized in Fig. 14. From an earlier study, we had known that introducing link adaptation inspired by the Hebbian principle in a frustrated system can result in it converging to a structurally balanced

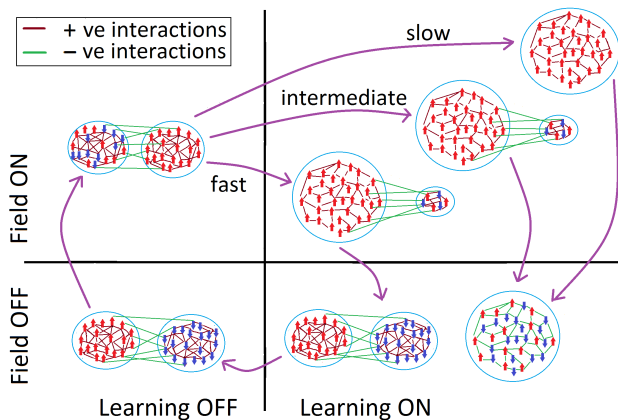


FIG. 14. Schematic representation of our key results. Starting from the structurally balanced network (with the different communities showing opposite ordering) at the bottom left quadrant, we obtain chimera state on introducing an external field of requisite strength (top left quadrant). Allowing the interactions to adapt with different learning rates result in the network maintaining balance but with different outcomes for the ordering. Fast and intermediate learning rates retain chimera order, although the disordered region is much diminished, while slow learning leads to complete order (top right quadrant). On withdrawing the field, the system subject to fast learning rate again converges to a structurally balanced network with oppositely ordered communities of approximately equal size, similar to the original network. Intermediate and slow learning, however, results in a fully frustrated network with complete disorder (bottom right quadrant).

state - corresponding to evolution of the underlying energy landscape - that depends on the initial state of the system. Applying this adaptation dynamics to a system exhibiting chimera order (as done in here) allows us to explore how the dynamics of the energy landscape is affected by an external field, as well as, asymmetry in the adaptation rule regarding negative and positive interactions.

We observe that when system is adapting through faster learning rates, the chimera order is maintained throughout its evolution, with the ordered module increasing in size at the expense of the disordered module. For slower learning rates, first the interactions of the elements belonging to the disordered module become weak which results in loss of chimera order. This is followed by the system converging to a fully ordered state where almost all the interactions are positive. The sizes of the two modules defining the system where one observes chimera order can be varied to see how the ratio of module sizes can affect the subsequent evolution of the system. Indeed, we see that the region in the field-temperature parameter space over which chimera order is seen increases as the ratio increases from 1. When the external field is withdrawn, the system returns to a structurally balanced state with modules of similar sizes if the adaptation rate is high. However, for slower learning rates, the system becomes completely frustrated.

We have also tried to explore how the structure of the energy landscape of the system evolves during learning.

Starting from a chimera ordered state that is subjected to adaptation rate and external field, we observe changes in the landscape after the field is switched off. Initially the system becomes completely frustrated. However, after an interval (which decreases with increasing learning rate) the system shows a sudden large increase in the basin of attraction of an energy minimum, although the frustration of the system has decreased only negligibly. This surprisingly radical change in the landscape resulting from relatively small degree of change in the interaction structure of the network is a question that needs to be explored further.

It is of interest to consider the implications of the results reported here for adaptation in biological systems. As connections in the brain evolve according to long-term potentiation that embodies the Hebbian principle that has inspired the link adaptation dynamics used in our study, it is natural to expect that the brain may exhibit at least some of the features observed here. Indeed, as mentioned earlier, the experimental observation of two dynamically anti-correlated subnetworks in the resting human brain [11] strongly suggests that in the absence of strong external stimulation the underlying network is structurally balanced. On the other hand, when exposed to stimuli, correlated brain activity is indeed observed - although not encompassing the entire network. This is, to some extent, reminiscent of the chimera ordered state that is seen in our model system. Thus, the brain may be seen as corresponding to a system subject to relatively fast adaptation rate. However, the Hebbian principle can apply to a much broader class of biological systems, e.g., gene regulation networks where the co-expression of genes has been suggested to result in their co-regulation over evolutionary time-scales [19]. As the adaptation in this case is provided by natural selection, which is orders of magnitude slower than the learning process in the brain mentioned earlier, it is probably not unreasonable to conclude that this can be seen as one corresponding to our model system subject to slow rate of adaptation. It is easy to see that the frustrated system with a large number of energy minima can be considered to be analogous to the cellular differentiation process that allows convergence to any one of a large number of possible cell fates dependent upon initial conditions. Indeed this analogy has been used earlier by Kauffman to motivate Boolean network models for explaining differentiation during biological development [20]. Extending this analogy, one may wonder whether the system has a state corresponding to the ordered state seen on exposing it to an external stimulus. As this state is unique and will be attained by the system independent of all initial conditions, it is tempting to suggest that induced pluripotency in cells exposed to chemical stimuli [21] may be the biological analogue. Therefore, it may be of interest to study the phenomena reported here in biologically realistic models of networks adapting at different time scales.

## ACKNOWLEDGEMENTS

We thank Rajeev Singh, Shakti N. Menon and R. Janaki for helpful discussions. This work was supported in part by IMSc Complex Systems Project (XII Plan)

funded by the Department of Atomic Energy, Government of India. The numerical work was carried out in machines of the IMSc High-Performance Computing facility, including “Satpura” which is partially funded by DST (Grant No. SR/NM/NS-44/2009).

- 
- [1] M. E. J. Newman, *Networks: An Introduction* (Oxford University Press, Oxford, 2010).
  - [2] A. Barrat, M. Barthélemy and A. Vespignani, *Dynamical Processes on Complex Networks* (Cambridge University Press, Cambridge, 2008).
  - [3] S. N. Dorogovtsev, A. V. Goltsev and J. F. F. Mendes, *Rev. Mod. Phys.* **80**, 1275 (2008).
  - [4] R. K. Pan and S. Sinha, *EPL* **85**, 68006 (2009).
  - [5] S. Dasgupta, R. K. Pan and S. Sinha, *Phys. Rev. E* **80**, 025101 (2009).
  - [6] J. A. Hertz, A. Krogh and R. G. Palmer, *Introduction to the Theory of Neural Computation* (Addison-Wesley, Redwood City, 1991).
  - [7] M. Mezard, G. Parisi and M. A. Virasoro, *Spin Glass Theory and Beyond* (World Scientific, Singapore, 1987).
  - [8] K. H. Fischer and J. A. Hertz, *Spin Glasses* (Cambridge University Press, Cambridge, 1991).
  - [9] D. Cartwright and F. Harary, *Psychol. Rev.* **63**, 277 (1956).
  - [10] F. Heider, *J. Psychol.* **21**, 107 (1946).
  - [11] M. D. Fox, A. Z. Snyder, J. L. Vincent, M. Corbetta, D. C. Van Essen and M. E. Raichle, *Proc. Natl. Acad. Sci. USA* **102**, 9673 (2005).
  - [12] R. Singh, S. Dasgupta and S. Sinha, *EPL* **95**, 10004 (2011).
  - [13] D. O. Hebb, *The Organization of Behavior* (John Wiley, New York, 1949).
  - [14] R. Singh, S. Dasgupta and S. Sinha, *EPL* **105**, 10003 (2014).
  - [15] G. Facchetti, G. Iacono and C. Altafini, *Proc. Natl. Acad. Sci. USA* **108**, 20953 (2011).
  - [16] J. J. Hopfield, *Proc. Natl. Acad. Sci. USA* **79**, 2554 (1982).
  - [17] N. Pradhan, S. Dasgupta and S. Sinha, *EPL* **94**, 38004 (2011).
  - [18] A. W. Bowman and A. Azzalini, *Applied Smoothing Techniques for Data Analysis* (Oxford University Press, Oxford, 1997).
  - [19] C. T. Fernando, A. M. L. Liekens, L. E. H. Bingle, C. Beck, T. Lenser, D. J. Stekel and J. E. Rowe, *J. R. Soc. Interface* **6**, 463 (2009).
  - [20] S. A. Kauffman, *Scientific American* **265** (2), 78 (1991).
  - [21] K. Takahashi and S. Yamanaka, *Cell* **126**, 663 (2006).